

# **MOLECULAR MODELLING OF CYP2F SUBSTRATES: COMPARISON OF NAPHTHALENE METABOLISM BY HUMAN, RAT AND MOUSE CYP2F SUBFAMILY ENZYMES**

David F.V. Lewis<sup>1\*</sup>, Yuko Ito<sup>2</sup>, and Brian G. Lake<sup>3</sup>

<sup>1</sup>*Faculty of Health and Medical Sciences, University of Surrey,  
Guildford, Surrey, UK*

<sup>2</sup>*Graduate School of Integrated Sciences, Division of Science of  
Biological Supramolecular Systems, Structural Bioinformatics,  
Yokohama City University, Yokohama, Kanagawa, Japan*

<sup>3</sup>*Centre for Toxicology, Faculty of Health and Medical Sciences,  
University of Surrey, Guildford, Surrey, UK*

## **SUMMARY**

We have constructed three-dimensional molecular models of some cytochrome P450 (CYP) CYP2F subfamily forms via homology with CYP2C5 where sequence identities are in the region of 55%, thus representing high degrees of confidence in the accuracy of the models produced. The three-dimensional structures of these CYP2F enzymes have been compared by molecular overlay, especially with regard to the active site regions, and it would appear that the substitution of a lysine (Lys-301) in human CYP2F1 for the usual glutamate (Glu-301) in mouse CYP2F2, goat CYPF3 and rat CYP2F4 prior to the conserved distal threonine residue may well constitute a significant factor in any species differences between these CYP2F enzymes. Both substrate binding to CYP2F2 and metabolic clearance by CYP2F enzymes correlate with the lipophilicity, parameter, log P (where P is

---

\* Author for correspondence:

David F.V. Lewis

Faculty of Health and Medical Sciences

University of Surrey

Guildford, Surrey, GU2 7XH, UK

e-mail: d.lewis@surrey.ac.uk

the octanol/water partition coefficient of the substrate). Other features of CYP2F substrate binding are likely to include  $\pi$ - $\pi$  stacking interactions between aromatic rings and hydrogen bonding in some cases.

The metabolism of the respiratory toxicant naphthalene is compared and contrasted between three mammalian species, namely mouse, rat and human. The CYPs involved in the metabolic activation and detoxification of naphthalene are discussed in the light of current evidence from both experimental and theoretical studies. It is noted that the CYP2F subfamily enzymes are associated with the activation of naphthalene in all three mammalian species, although there are marked differences between man and the two rodent species in the toxicity of this compound.

### KEY WORDS

cytochromes P450, CYP2F enzymes, naphthalene, QSARs

### INTRODUCTION

There is considerable current interest in the roles of the cytochrome P450s (CYPs) in the activation and detoxification of xenobiotics /1-8/. The respiratory tract of rodents, non-human primates and humans contains a range of CYP forms, including CYP2F subfamily forms /9-14/.

Many studies have demonstrated that respiratory tract CYP forms can bioactivate xenobiotics to toxic and carcinogenic metabolites. For example, naphthalene is bioactivated by CYP2F2 present in mouse Clara cells to naphthalene 1,2-epoxide. Although naphthalene produces Clara cell toxicity in the mouse, it does not produce such lesions in the rat /11,15/. Repeated administration results in a tolerance to naphthalene-induced mouse Clara cell toxicity, which is attributable to increased levels of reduced glutathione /16/. Apart from Clara cells, CYP2F forms have been shown to be present in the olfactory

---

**Abbreviations:** CYP = cytochrome P450;  $K_m$  = Michaelis constant for the enzyme-catalyzed reaction; SRS = substrate recognition site; P = octanol/water partition coefficient, NNK = 4-(methylnitrosamino)-1-(3-pyridyl)-1-butanone.

epithelium of rats, mice and non-human primates /9,10/ and naphthalene has been shown to produce toxicity in the olfactory epithelium of both rats and mice /11,17/. Naphthalene inhalation bioassays have demonstrated the formation of pulmonary alveolar/bronchiolar adenomas in female mice and nasal respiratory epithelium adenomas and olfactory epithelium neuroblastomas in rats /11,17,18/. The mode of action for naphthalene-induced rodent respiratory tract tumour formation appears to involve cytotoxicity leading to cellular injury and increased cell replication rates /11/.

CYP2F subfamily enzymes which can metabolise naphthalene include human CYP2F1, mouse CYP2F2 and rat CYP2F4 /10,11, 13,19/. CYP2F3 is the goat orthologue of these enzymes, and some substrate binding studies have been conducted on this form, such as for 3-methylindole /20/. It is interesting to note that the  $K_m$  value for 3-methylindole metabolism via CYP2F1 at 18  $\mu\text{M}$  represents a tighter binding energy than that found for the CYP2F3 orthologue where the  $K_m$  value is 340  $\mu\text{M}$  /20/.

In a previous modelling study we generated a homology model of the mouse CYP2F2 enzyme based on the bacterial CYP102 crystallographic template /21/. In this work, we have utilized the relatively recently reported crystal structure of rabbit CYP2C5 /22/ to construct homology models of CYP2F1, CYP2F2 and CYP2F4. These enzyme models have been probed with a number of selective CYP2F substrates, including naphthalene, and a substrate template appears to fit all three enzymes satisfactorily. Consequently, it is expected that there would be relatively few differences in substrate selectivity between these orthologous enzymes.

## METHODS

An alignment (see Fig. 1) between the template sequence CYP2C5 of known crystal structure /22/ and the target sequences of CYP2F1, CYP2F2, CYP2F3 and CYP2F4 was constructed using the BLAST procedure and edited slightly to maintain conservation of secondary structural elements ( $\alpha$ -helices and  $\beta$ -sheets) in the template structure /22/. The multiple sequence alignment of the substrate recognition sites (SRSs) is shown in Table 1. SRS is a term coined by Gotoh /23/ based on sequence comparisons in the CYP2 family. Homology models for each CYP2F enzyme were produced via the Sybyl

**TABLE 1**  
Substrate recognition sites (SRs) in CYP2F and CYP2C5

[illegible]

SRS4												
•	I	A	V	S	D	L	F	G	A	G	*	
2C5											T	S
2F1	M	T	T	H	N	L	L	F	G	G	T	S
2F2	M	T	T	H	N	L	L	F	G	G	T	G
2F3	M	T	T	H	N	L	L	F	G	G	T	G
2F4	M	T	T	H	N	L	L	F	G	G	T	G
SRS5												
•	I	A	L	L	P	T	N	L	P	H	*	
2C5												365
2F1	A	T	I	I	P	M	N	L	P	H		369
2F2	A	T	V	I	P	M	N	L	P	H		369
2F3	A	T	I	I	P	M	S	L	P	H		369
2F4	A	T	V	I	P	M	N	L	P	H		369
SRS6												
•	I	D	A	V	V	N	*	F	V	S		475
2C5												
2F1	L	D	P	L	S	S	G	L	G	N		479
2F2	L	D	P	L	S	S	G	L	G	N		479
2F3	L	D	P	L	S	S	G	L	G	N		479
2F4	L	D	P	L	S	S	G	L	G	N		479

\* = invariant residue; • = conserved residue.

2C5	1:--MDP-VVVLV-LGLCCLLLL-SIWKQNSGRGKLPFGPTFPFIIGNILQIDAKDISKSLT	55
2F1	1:MDSISTAILLLLLLALVOLLTLTSS-RD---KGLPFGPRPLSILGNLLCSQDMLTSLT	56
2F2	1:MDGVSTAILLLLLLAVISLSLTSS-RG---KGLPFGPKPLPILGNLLQLRSQDLTSLT	56
2F3	1:MDSISTAILLLLLLALICLLTLTSS-KG---KGLPFGPRALPFLGNLLQLRSQDMLTSLT	56
2C5	56:KFSECYGVPVFTVVLGMKPTVVLHGVEAVKEALVDLGEFAGRGSVPILEKVKSGLGIAFS	115
2F1	57:KLSKEYGSMYTVHLGPRRVVVLSGYQAVKEALVDQGEFSGRGDYPAFFNFTKNGGIAFS	116
2F2	57:KLSKEYGSMYTVHLGSRPVVVLSGYQTVKEALVDKGEFSGRGAYPVPFFNFTKNGGIAFS	116
2F3	57:KLSKEFGAVYTVHLGPRRVVVLSGYQAVKEALVDQAEFSGRGDYPAFFNFTKNGGIAFS	116
2C5	116:NAKTWKEMRRFSLMTLRNFGMGKRSIEDRIQEEARCLVEELRKTNASPCDPTFILGCAPC	175
2F1	117:SGDRWKVLROFSIQILRNFGMGKRSIEERILEEGSFLLADVRKTEGEPDPTFVLSRSVS	176
2F2	117:DGERWKILRRFSVQILRNFGMGKRSIEERILEEGSFLLLEVLRKMEGKFPDPTFVLSRSVS	176
2F3	117:NGDRWKALKKYSIQILRNFGMGKRTIEERILEEGHFLLEELRKTQGKFPDPTFVLSRSVS	176
2C5	176:NVICSVIFHNRFDYKDEEFLKLMESLNENVRILSSPWLQVYNN---FPALLDYEPGLIK	231
2F1	177:NIICSVLFGSRFDYDDERLLTIIRLINDNFQIMSSPWGELYDILDPRFPSSLDDWVPGPHQ	236
2F2	177:NIICSVVFGSRFDYDDERLLTIHFINDNFQIMSSPWGEMYN---FPSVLDWIIPGPHK	232
2F3	177:NIICSVLFGSRFDYDDERLLTIHILINENFQIMSSPWGEMYN---FPNLLDWVPGPHR	232
2C5	232:TLLKNADYIKNFIMEKVKHEQKLLDVNNPRDFIDCFLTKMEQENN--LE-FTLESIVIAV	288
2F1	237:RIFQNEFKCLRDILTAHSVHDHQASS---PRDFIQCFLLTKMAEEKDPLSHFMDTLTLLMT	292
2F2	233:RLFRNFGGKMDLARSVREHQDSLDPNSPRDFIDCFLTKMAQEKQDPLSHENMDTLTLLMT	292
2F3	233:RLEKNYGRMKNLARSVREHQASLDPSPRDFIDCFLTKMAQEKQDPLSHFMDTLTLLMT	292
2C5	289:SDL-FGAGTETTTSTTLRYSLLLLLKHPEVAARVQEETERVIGRHRSPCMQDRSRMEPYTDA	347
2F1	293:HNLLFGG-TKTVSTTLHHAFLALMKYPKVQARVQEEIDLVVGRARLPALKDRAAMEPYTDA	351
2F2	293:HNLLFGG-TETVGTTLRHAFILMKYPKVQARVQEEIDRVVGRSRMPTLEDRTSMETPYTDA	351
2F3	293:HNLLFGG-TETVGTTLRHAFRLMKYPEVQVRVQEEIDRVVGRERLPTVEDRAEMPYTDA	351
2C5	348:VIHEVQRFIDLLPTNLPHAVTRDVRFRNYFIPKGTDIITSLTSVLHDEKAFNPKNKVFDPG	407
2F1	352:VIHEVQRFADIIIPMNLPHRVTRDTAFRGFLIPKGTDVITLLNTVHYDPSQFLTPQEFNPE	411
2F2	352:VIHEVQRFADVPIPMNLPHRVTRDTPFRGFLIPKGTDVITLLNTVHYDPSQFLTPQEFNPE	411
2F3	352:VIHEVQRFADIIIPMSLPHRVTRDTNFRGFLIPKGTDVITLLNTVHYDPSQFLTPQEFNPE	411
2C5	408:HFLDESGNFKKSDYFMFFSAGKRMVGEGLARMELFLFSLTILQNFKLQSLVEPKDLDT	467
2F1	412:HFLDANQSFKKSPAEMFFSAGRRCLGELLARMELFLYLTAILOSFSLQPLGAPEDIDLT	471
2F2	412:HFLDONHSFKKSPAEMFFSAGRRCLGELPLARMELFIYFTSILQNFLLQPLVDPEDIDLT	471
2F3	412:HFLDANMSFKKSPAEMFFSAGRRCLGEALARMELFLYLTAILOSFSLQPLGAPEDIDLT	471
2C5	468:AVVNGFVSVPSPSYQLCFIPI	487
2F1	472:PLSSGLGNLPRPFQLCLRPR	491
2F2	472:PLSSGLGNLPRPFQLCMHIR	491
2F3	472:PLSSGLGNVPRPYQLCVRAR	491

**Fig. 1:** Multiple sequence alignment of CYP2C5 with four CYP2F subfamily proteins: CYP2F1 (human), CYP2F2 (mouse), CYP2F3 (goat) and CYP2F4 (rat).

Biopolymer software (Tripos Associates, St. Louis, MO) using the method of residue replacement based on the multiple sequence alignment. All additional residues in the target sequences were added via loop-searching of the protein database using Sybyl Biopolymer algorithms. The resulting raw 3-D structures were energy minimized using molecular mechanics via the Tripos force field for 100 iterative cycles such that low minimum energy geometries were obtained. The final, relaxed CYP2F structures were then probed with naphthalene and other typical CYP2F substrates using the AutoDock software, prior to molecular dynamics (MD) simulations. Lipophilicity relationships between log clearance and log P (where P is the experimentally-determined octanol/water partition coefficient) were calculated using the GraphPad Software package (GraphPad Software, Inc., San Diego, California).

## RESULTS AND DISCUSSION

### (a) Molecular modelling and QSARs

The homology models of CYP2F1 (human), CYP2F2 (mouse) and CYP2F4 (rat) minimized smoothly over 100 iterative cycles of molecular mechanics to give low energy geometry conformations and the relevant minimum energies were, respectively,  $-1087.261 \text{ kcal.mol}^{-1}$  (CYP2F1),  $-1213.311 \text{ kcal.mol}^{-1}$  (CYP2F2) and  $-1233.513 \text{ kcal.mol}^{-1}$  (CYP2F4) as shown in Table 2. Typical substrates for CYP2F subfamily enzymes were found to dock satisfactorily within the putative active sites in each case. The most common interactions between substrates and the enzymes were hydrogen bonding and aromatic  $\pi$ - $\pi$  stacking between complementary groupings on the substrates and key amino acid residues lining the haem pocket.

Figure 2 shows a view of the putative active site region of CYP2F1 containing the substrate, naphthalene, orientated for 1,2-epoxidation, which is consistent with experimental findings.

There are two phenylalanines (Phe-206 and Phe-297) present in the CYP2F enzyme active sites at ideal locations for  $\pi$ - $\pi$  stacking with naphthalene and other related substrates. In addition, two serines (Ser-474 and Ser-475) in SRS6 (SRS = substrate recognition site) may form one or more hydrogen bonds with polar substrates such as NNK

TABLE 2

Comparison between homologies, final energies, naphthalene metabolism rates and active site residue 301 for CYP2F1, CYP2F2 and CYP2F4 enzymes

CYP	Identity with CYP2C5	Minimized energy <sup>a</sup> (kcalmol <sup>-1</sup> )	Rate <sup>b</sup> (nmol/min/nmol P450)	Residue at position 301
2F1	53%	-1087.261	0.004*	K (Lys)
2F2	56%	-1213.311	104	E (Glu)
2F4	56%	-1233.513	107	E (Glu)

<sup>a</sup> Based on 100 iterative cycles of molecular mechanics using the Tripos force field.

<sup>b</sup> Based on naphthalene metabolism by CYP2F enzyme /13/.

\* For the formation of 1R,2S-naphthalene epoxide.



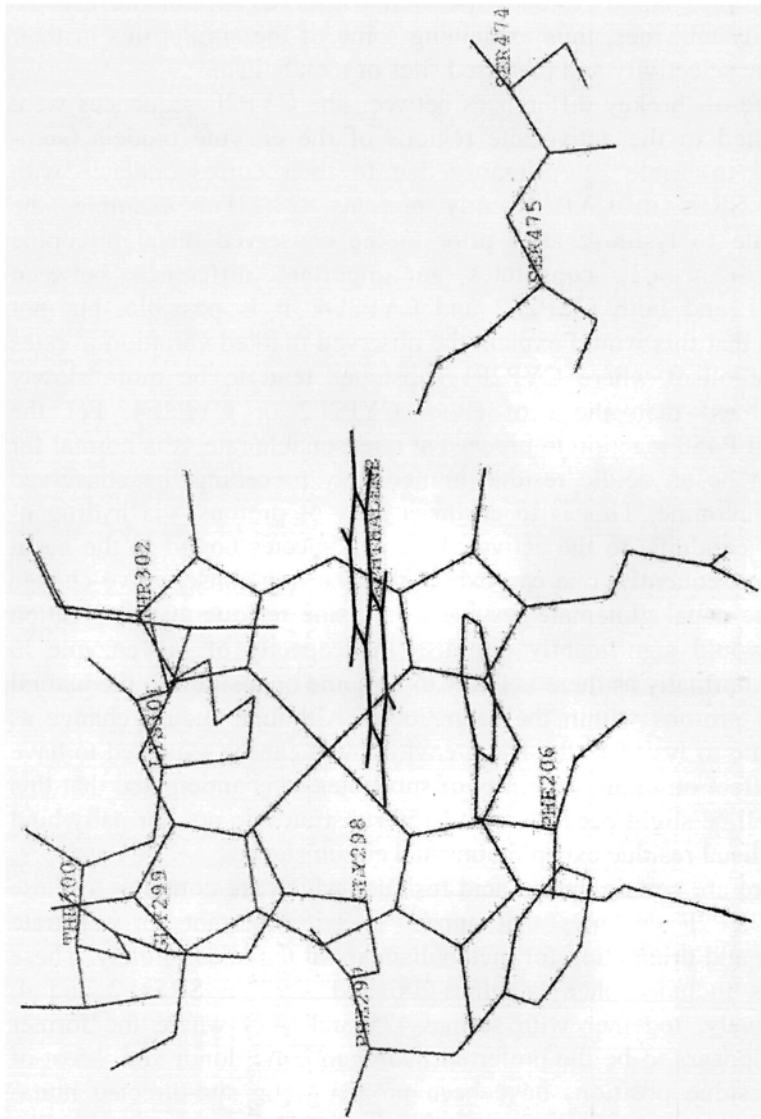


**Fig. 2:** A view of the putative active site of CYP2F1 showing the substrate, naphthalene, orientated for 1,2-epoxidation.

(4-(methylnitrosamino)-1-(3-pyridyl)-1-butanone), ipomeanol and 4-nitrophenol. There is also the possibility of weak hydrogen bonding to aromatic rings which could occur in the case of naphthalene binding, for example. These residues are well conserved within the CYP2F subfamily enzymes, thus explaining some of the similarities in their substrate selectivity and preferred sites of metabolism.

Some of the key differences between the CYP2F sequences were manifested in the active site regions of the enzyme models (summarized in Table 3), primarily due to their correspondence with known SRSs in CYP2 family proteins [23]. For example, the glutamate to lysine change prior to the conserved distal threonine residue (Thr-302) constitutes an important difference between CYP2F1 and both CYP2F2 and CYP2F4. It is possible, but not certain, that this would explain the observed marked variation in rates of metabolism where CYP2F1 substrates tend to be more slowly metabolized than those of either CYP2F2 or CYP2F4. For the standard P450 reaction to proceed at a reasonable rate, it is normal for there to be an acidic residue immediately preceding the conserved distal threonine. This is to ensure a flow of protons, via hydrogen-bonded conduits, to the activated oxygen species bound to the haem iron. Consequently, one can expect that the non-conservative change from the usual glutamate residue to a lysine residue at this position (301) would significantly diminish the capacity of the enzyme to operate normally as there is likely to be some opposition to the natural flow of protons within the haem locus. Although such a change as glutamate to lysine in the haem environment can be expected to have some effect on binding affinity of substrates, it is anticipated that this may well be slight because most P450 substrates do not normally bind to this distal residue except in unusual circumstances.

There are certain amino acid residues which are common to these three CYP2F enzymes that appear to be important for substrate binding and orientation for metabolism about the haem moiety. These residues include: phenylalanines-206 and -297 in SRSs 2 and 4, respectively, together with serines-475 and -474 where the former serine appears to be the preferred hydrogen bond donor site. Most of these residue positions have been probed using site-directed mutagenesis experiments in other CYP2 family enzymes but not in the CYP2F family. Nevertheless, it is likely that they do indeed occupy the substrate binding sites of the CYP2F enzymes under current

TABLE 3  
Key differences in CYP2F sequences in SRS regions

Position	CYP2F1	CYP2F2	CYP2F4	Comment	SRS region
100	D	A	S	Non-conservative change	1
103	A	V	I	Conservative change	1
109	K	R	K	Conservative change	1
117	S	D	D	Non-conservative change	1
200	R	H	H	Conservative change	2
201	L	F	F	Non-conservative change	2
207	Q	K	Q	Non-conservative change	2
236	Q	R	R	Non-conservative change	3
239	K	G	G	Non-conservative change	3
301	K	E	E	Non-conservative change	4
304	S	G	G	Non-conservative change	4
362	I	V	V	Conservative change	5

SRS = substrate recognition site /23/.

investigation, and their conservation within this subfamily can be expected to explain the broadly similar  $K_m$  values for substrates binding to either CYP2F1, CYP2F2 or CYP2F4. There are, in general, fewer differences between CYP2F2 and CYP2F4 in the SRS (4 changes) relative to those between CYP2F1 and the two rodent forms (9 changes).

Based on an analysis of the available experimental data on  $K_m$  and  $V_{max}$  values for CYP2F1, CYP2F2 and CYP2F4 substrates, as shown in Tables 4, 5 and 6, it has been possible to formulate some simple linear relationships with biological activity and the compound lipophilicity parameter  $\log P$ , where  $P$  is the octanol/water partition coefficient. There is a linear relationship between  $\log$  Rate (or  $\log V_{max}$ ) and  $\log P$  for a combined set of CYP2F2 and CYP2F4 substrates, with a correlation coefficient ( $R$ ) of 0.91 ( $R^2 = 0.83$ ); whereas a somewhat weaker linear correlation is apparent for CYP2F1 substrates which is, nevertheless, of similar slope to the former. These give two parallel lines, therefore, as lipophilicity plots. The generally lower rates of CYP2F1-mediated substrate metabolism relative to those of both CYP2F2 and CYP2F4 could be due to the non-conservative change glutamate to lysine in SRS4, as described previously. Where data for CYP2F2 solely are considered, the correlation with  $\log P$  increases slightly to give  $R = 0.93$  ( $R^2 = 0.87$ ) although the slope and intercept on the  $y$  axis are similar.

For CYP2F2 substrates, there is a good correlation between  $\log K_m$  and  $\log P$ . When converted to  $\Delta G_{bind}$  and  $\Delta G_{part}$  values, respectively, it appears that the magnitude of the correlation improves with the exclusion of naphthalene, indicating that this substrate is a clear outlier. The correlation coefficient with five compounds, including naphthalene, is 0.94 ( $R^2 = 0.89$ ) whereas, when the naphthalene data are removed, the coefficient increases significantly to 0.996 ( $R^2 = 0.99$ ). The  $y$ -intercept of this correlation at  $-1.7 \text{ kcal.mol}^{-1}$  suggests that the common interactions between substrates and CYP2F are likely to be either hydrogen bonding or two aromatic  $\pi$ - $\pi$  stacking contacts of  $-0.85 \text{ kcal.mol}^{-1}$  each, which is in good agreement with the average literature value of  $-0.9 \text{ kcal.mol}^{-1}$ .

However, the clearance data ( $Cl = V_{max}/K_m$ ) for seven substrates of CYP2F1, CYP2F2 and CYP2F4 combined show an excellent correlation with  $\log P$  when they are expressed in logarithmic form. In this case, the correlation coefficient is 0.997 ( $R^2 = 0.994$ ) and the line

TABLE 4

Substrate metabolism  $K_m$  values ( $\mu\text{M}$ ) for CYP2F enzymes and lipophilicity data

Compound	CYP2F1	CYP2F2	CYP2F4	log P
3-Methylindole	18			2.60
Benzene	3.8			2.13
Naphthalene		3	3	3.37
1-Nitronaphthalene		21.5	18	3.19
2-Methylnaphthalene		3.7		3.86
1,1-Dichloroethene		254	5600	2.13
Trichloroethene		114	64	2.61

$$\Delta G_{\text{bind}} = RT \ln K_m$$

where R is the gas constant and T is the absolute temperature (310K).

$$\Delta G_{\text{part}} = -RT \ln P$$

where R is the gas constant and T is the absolute temperature (310K).

For the CYP2F2 substrates, excluding the naphthalene outlier, we have:

$$\Delta G_{\text{bind}} = 1.087 \Delta G_{\text{part}} - 1.712$$

$$(\pm 0.070)$$

$$n = 4; s = 0.1284; R = 0.9959; R^2 = 0.9918; F = 242.403$$

For all five CYP2F2 substrates, we get the following correlation:

$$\Delta G_{\text{bind}} = 1.208 \Delta G_{\text{part}} - 1.374$$

$$(\pm 0.247)$$

$$n = 5; s = 0.4719; R = 0.9427; R^2 = 0.8887; F = 23.950$$

Reference for  $K_m$  data: Zhang and Ding /13/.

TABLE 5

Clearance (Cl) of CYP2F substrate metabolism and log P data

Substrate	CYP	$V_{\max}^*$	$K_m$ ( $\mu$ M)	$V_{\max}/K_m^{\dagger}$	log Cl	log P
3-Methylindole	2F1	1.3	18	0.0722	4.8587	2.60
Benzene	2F1	0.01	3.8	0.0026	3.4202	2.13
Naphthalene	2F2	104	3	34.6667	7.5399	3.37
1-Nitronaphthalene	2F2	17.1	21.5	0.7953	5.9006	3.19
2-Methylnaphthalene	2F2	67.6	3.7	18.2703	7.2617	3.86
1,1-Dichloroethene	2F2	2.8	254	0.0110	4.0423	2.13
Trichloroethene	2F2	13	114	0.1140	5.0570	2.61
Naphthalene	2F4	107	3	35.6667	7.5523	3.37
1-Nitronaphthalene	2F4	25	18	1.3889	6.1427	3.19
Trichloroethene	2F4	17	64	0.2656	5.4243	2.61
1,1-Dichloroethene	2F4	74	5600	0.0132	4.1210	2.13

\* Units are nmol/min/nmol P450.

Cl =  $V_{\max}/K_m$  (intrinsic clearance). $\dagger$  Units are ml/min/nmol P450.

For the CYP2F2 substrates apart from naphthalene, 3-methylindole (2F1) and 1-nitronaphthalene and 1,1-dichloroethene in CYP2F4, we have:  $\log Cl = 1.835 (\pm 0.064) \log P + 0.173$ ;  $n = 7$ ;  $s = 0.0987$ ;  $R = 0.9970$ ;  $R^2 = 0.9940$ ;  $F = 829.585$ .

When just the CYP2F2 substrates (apart from naphthalene) are considered, we find:

$\log Cl = 1.820 (\pm 0.086) \log P + 0.201$ ;  $n = 4$ ;  $s = 0.1117$ ;  $R = 0.9978$ ;  $R^2 = 0.9955$ ;  $F = 453.046$ .

Reference for biological data: Zhang and Ding /13/.

**TABLE 6**  
Stereoselectivity of naphthalene activation via CYP2F forms

Species	Lung microsomes 1R,2S:1S,2R ratio	CYP2F	Expressed enzymes 1R,2S:1S,2R ratio	$V_{\max}^{\dagger}$	$K_m$ ( $\mu$ M)
<b>Human</b>	0.85	2F1	0.13	0.004 (RS form) 0.031 (SR form)	N/A
<b>Mouse</b>	10 (30*)	2F2	66	104	3
<b>Rat</b>	$\leq 1.3$	2F4	>50	107	3

$\dagger$  Units are nmol/min/nmol P450.

\* At low concentrations.

N/A = data not available.

appears to go through the origin. When only CYP2F2 substrates are considered, the correlation is of a similar nature with a correlation coefficient of 0.998 ( $R^2 = 0.996$ ) and also apparently passing through zero. On the basis of these findings from QSAR analysis, one can conclude that lipophilic character plays a major role in explaining differences in substrate binding affinity, rate and clearance in CYP2F substrates and that the  $\pi$ -character of the compounds concerned is important for binding to the enzymes' active sites, although hydrogen bonding may also be involved.

CYP2F substrates include naphthalene, styrene, 3-methylindole, 4-ipomeanol, trichloro-ethene, benzene and dichloroethene /12,14, 24-32/. Figures 3 and 4 present schemes for the metabolism of naphthalene, as an example of a typical CYP2F substrate.

Naphthalene is metabolized to the 1,2-epoxide by CYP2F1 and to 1-naphthol by CYP2A13 and CYP2B6, although it is possible that other enzymes may also be involved /7,33-35/. It is likely that the mechanisms of naphthalene metabolite formation are different between the CYP2F1- and CYP2B6-mediated pathways. CYP2A13 also catalyzes the 2-hydroxylation of naphthalene, and this is an enzyme found in the respiratory tract as is the case for CYP2F1, whereas CYP2B6 is a hepatic form. In addition, there are species differences in naphthalene metabolism which suggest that CYP2F2 may be more effective in forming the epoxide in mice rather than the situation in man involving CYP2F1. Unfortunately, very few  $K_m$  values for CYP2F substrates have been reported in the scientific literature thus far, although some data on 3-methylindole are available, as mentioned below.

### (b) 3-Methylindole metabolism via CYP2F enzymes

There are differences in  $K_m$  values for 3-methylindole metabolism between humans and goat /20/. For 3-methylindole the  $K_m$  value 18  $\mu\text{M}$  is via the CYP2F1 enzyme. There is a lysine residue just before the distal threonine in CYP2F1 and one can show that, in this case,  $\Delta G_{\text{bind}} = -6.73 \text{ kcal.mol}^{-1}$ . However, there is a glutamate before the distal threonine in CYP2F3 and, in this case,  $\Delta G_{\text{bind}} = -4.92 \text{ kcal.mol}^{-1}$ , as the  $K_m$  value is 340  $\mu\text{M}$  for 3-methylindole metabolism in the goat. The energetic differences between lysine and glutamate in substrate binding can be estimated /36/, although it is likely that such a change



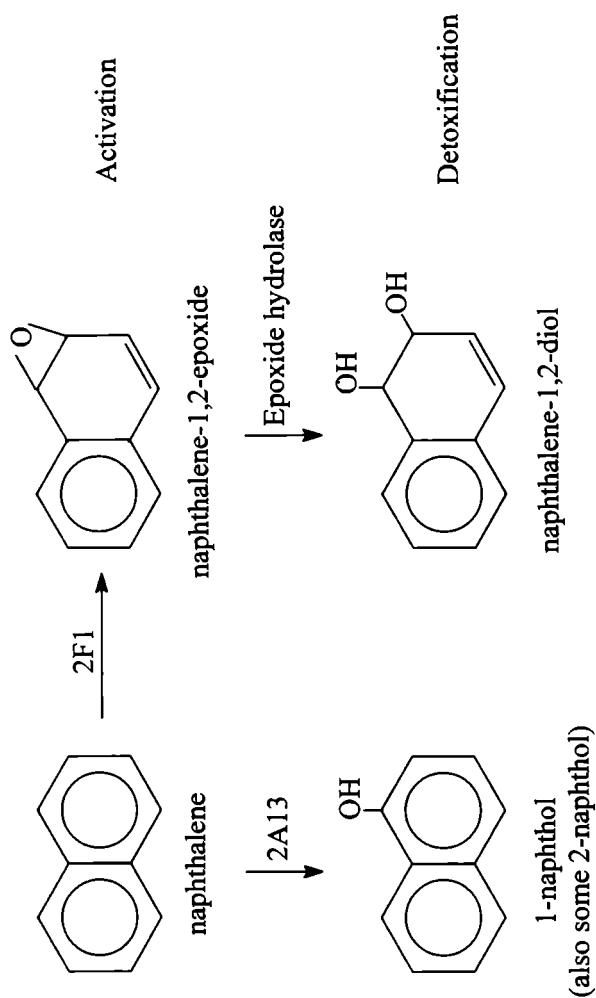
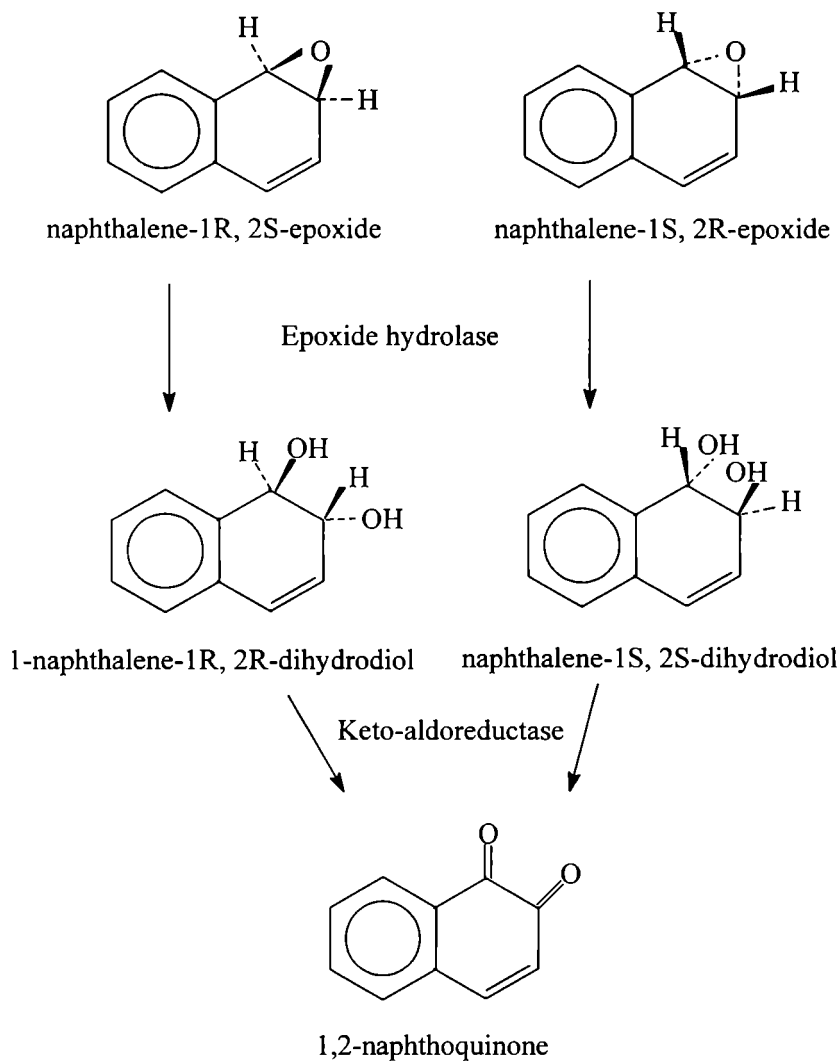


Fig. 3: Phase I metabolism of naphthalene in humans.



**Fig. 4:** Metabolism of the 1,2-epoxides of naphthalene. NB: Epoxide hydrolase preferentially attacks the less-hindered carbon on the epoxide.

may affect the rate of substrate metabolism rather than binding affinity.

There could be a strong desolvation aspect to CYP2F substrate binding as 3-methylindole is known to be fairly lipophilic (for 3-methylindole, its  $\log P = 2.60$ ) so the rest of the interaction energy is probably due to  $\pi$ - $\pi$  stacking, with one  $\pi$ - $\pi$  interaction in CYP2F3 and maybe two or three  $\pi$ - $\pi$  stacks in CYP2F1, if sufficient aromatic residues are present within the active site. The  $\log P$  value of 2.60 for 3-methylindole implies a partitioning energy,  $\Delta G_{\text{part}}$ , of  $-3.688 \text{ kcal.mol}^{-1}$  and, consequently, a simple calculation, based on the  $\Delta G_{\text{bind}}$  values for CYP2F3- and CYP2F1-mediated metabolism of 3-methylindole indicates that the non-lipophilic interactions are  $-1.232$  and  $-3.042 \text{ kcal.mol}^{-1}$ , respectively, which is consistent with one aromatic  $\pi$ - $\pi$  stacking interaction in CYP2F3 and as many as three  $\pi$ - $\pi$  stacks in CYP2F1. However, one would need to investigate the active sites of these enzymes, as the change from glutamate to lysine prior to the distal threonine could well be an important factor, and the sidechain of lysine would also be expected to show a somewhat higher hydrophobicity than that of glutamate. Moreover, this non-conservative change could well explain the significantly slower rate of naphthalene epoxidation via CYP2F1, relative to that of CYP2F2 and CYP2F4 enzymes, which display similar rates.

### (c) CYP2B-mediated naphthalene metabolism

Naphthalene is metabolized to 1-naphthol by CYP2B6 in humans and, consequently, this detoxifying pathway may also occur in rodent species mediated via CYP2B enzymes. For the CYP2B subfamily, the mouse forms are CYP2B9, CYP2B10 and CYP2B13, of which CYP2B9 is the major enzyme. The rat forms are CYP2B1, CYP2B2 and various others of minor importance are also known, namely CYP2B3, CYP2B12, CYP2B14, CYP2B15 and CYP2B16 [37]. However, CYP2B1 is the major CYP2B subfamily enzyme in this species, and this has been extensively studied for many years. Both CYP2B1 and CYP2B2 are inducible by phenobarbital, leading to the description of these enzymes as the PB-inducible forms. The human form of CYP2B is CYP2B6 and this represents the only CYP2B subfamily enzyme in man (representing about 5% of the total hepatic P450 on average). This has a rather limited involvement in the metabolism of foreign compounds in humans, however, in comparison

with the more important roles of CYP2B subfamily enzymes in the rat and mouse. Consequently, it is unlikely that enzymes of the CYP2B subfamily contribute significantly to the metabolism of naphthalene in the respiratory tract, irrespective of the species under consideration.

#### **(d) Comparison between naphthalene and coumarin**

Table 7 summarizes metabolic and physicochemical data for naphthalene in comparison with that of the structurally-related compound, coumarin, which may also be a CYP2F substrate /38/. The two compounds are clearly structurally related, both can form cytotoxic epoxides and it is known that Clara cell toxicity is a feature of both naphthalene and coumarin toxicology /11,39-41/. Like naphthalene, tolerance to Clara cell injury is observed after repeated dosing of coumarin /42/. Coumarin has also been shown to produce toxicity in the olfactory mucosa of mice and rats, where CYP2G1 appears to be involved in metabolic activation /43/. For coumarin and naphthalene there are also detoxifying pathways of metabolism which lead to hydroxylated forms of the parent compounds, which are thus able to become readily conjugated and excreted. It is possible, therefore, that the overall toxicity of coumarin and naphthalene in different mammalian species results from the relative balance between activating and detoxifying pathways, the number of Clara cells in lung tissue, together with the level of competence of the natural defence systems (e.g. cellular glutathione) present in the species concerned.

#### **(e) Species differences in naphthalene epoxidation via CYP2F**

Naphthalene produces Clara cell injury in the mouse but not in the rat, whereas rats appear to be more sensitive than mice to olfactory epithelium toxicity /11,17/. Activation is generally thought to be due to the formation of the 1,2-epoxide, which can then give rise to the 1,2-diol which forms 1,2-naphthoquinone or undergoes further epoxidation at the 3,4-position, thus producing the 1,2-diol-3,4-epoxide /11/. It is believed that the initial epoxidation step is primarily mediated by CYP2F enzymes, although it is possible that other P450s may also mediate naphthalene epoxidation in these mammalian species, such as CYP1A2 /33/. There are two stereoisomers of the 1,2-epoxide of naphthalene and the ratio of these two isomers exhibits species variation between rat, mouse and man. Data for the

stereoselectivity towards the two naphthalene 1,2-epoxides and rates of formation of these epoxides by CYP2F enzymes are summarized in Table 6. In general, the pattern shows that there is a preference for the 1S,2R-epoxidation in man and via CYP2F1, whereas both CYP2F2 and CYP2F4 preferentially give rise to the 1R,2S-epoxide, which is broadly mirrored in the whole animal data. In addition, there are marked differences in the rates of naphthalene epoxidation between the three species. While the mouse and rat exhibit fairly similar values for both  $K_m$  and  $V_{max}$ , the rate of naphthalene epoxidation is much lower with human CYP2F1. In one study with expressed CYP2F1 the rate of naphthalene metabolism was less than 0.1% of the rate of metabolism observed with mouse CYP2F2 /14/. The rate of 1S,2R-epoxidation via CYP2F1 is roughly seven times greater than that of 1R,2S-epoxide formation, suggesting that the orientation of naphthalene in the CYP2F1 active site tends to favour the formation of one stereoisomer. Presumably, this is brought about by naphthalene binding to certain key active site residues, including, for example, any phenylalanine side-chains close to the haem moiety, as mentioned previously.

Inspection of the SRS regions of the relevant CYP2F enzymes indicates that there are only nine residue positions where the sequence changes between the three orthologues (see Table 3). For differences between CYP2F2 (mouse) and CYP2F4 (rat), it appears that only four SRS residues are changed between the two rodent species, and the majority of these are in SRS1 (see Table 3). The most likely candidate residue for explaining differences in naphthalene metabolism (namely, stereoselectivity and rate of metabolism) between man and the two rodent species is Lys-301 in CYP2F1, which undergoes a non-conservative change to Glu-301 in CYP2F2 and CYP2F4. There are several other possibilities, however, which should also be taken into consideration. For example, Phe-201 in CYP2F1 is not conserved in CYP2F2 and CYP2F4 sequences, where it becomes Leu-201, and this may affect the orientation and binding affinity of naphthalene within the haem locus. Furthermore, it is important to recognize that the 1R,2S-epoxide is more rapidly converted to the diol than the 1S,2R-form and studies with isolated mouse hepatocytes have demonstrated that 1S,2R-epoxide is more toxic than the 1R, 2S-form /11/.

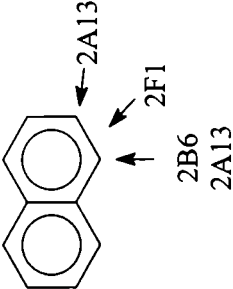
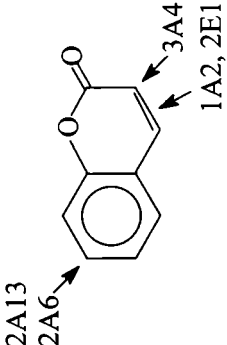
Differences in the structure of CYP2F1 compared to CYP2F2 and CYP2F4, which result in lower rates of naphthalene bioactivation by

TABLE 7

Comparison between physicochemical and biochemical properties of coumarin and naphthalene

Compound	Naphthalene	Coumarin
<b>Formula</b>	$C_{10}H_8$	$C_9H_6O_2$
<b>M<sub>r</sub></b>	128.17	146.15
<b>log P</b>	3.37	1.39
<b>Human CYPs involved</b>	CYP2F1, CYP2A13, CYP2B6 and others	CYP2A6, CYP1A2, CYP2E1 and CYP3A4
<b>K<sub>m</sub></b>	Not known	0.3 $\mu$ M (CYP2A6) to 6 $\mu$ M (CYP2A6)
<b>Metabolism</b>	1,2-epoxidation (CYP2F1) 1-hydroxylation (CYP2B6 and CYP2A13) 2-hydroxylation (CYP2A13)	7-hydroxylation (CYP2A6) 3,4-epoxidation (CYP1A2, CYP2E1) 3-hydroxylation (CYP3A4)
<b>Rodent respiratory tract toxicity</b>	Mouse lung Clara cell and nasal olfactory epithelium toxicity, rat respiratory and nasal olfactory epithelium toxicity	Mouse lung Clara cell toxicity, rat and mouse olfactory mucosa toxicity
<b>Rodent carcinogenicity</b>	Mouse lung tumours, rat respiratory and olfactory epithelium tumours	Mouse lung tumours
<b>Species differences</b>	Toxicity greater in rodents than in human	Toxicity greater in rodents than in human
<b>References</b>	/14,21,49/	/40,41/43,50/

Table 7 continued

Compound	Naphthalene	Coumarin
Structure (showing sites of metabolism)	 <p>2A13 2F1 2B6 2A13</p>	 <p>2A13 2A6 3A4 1A2, 2E1</p>
Active site interactions	$\pi$ - $\pi$ stacking	$\pi$ - $\pi$ stacking and hydrogen bonding
Steric and electronic factors	Both are in operation but electronic is probably greater as hydrogen bonding is not likely to occur	Both are in operation but steric is probably greater due to the hydrogen bonding component

the human CYP2F form, thus constitute an important species difference between humans and rodents. However, other factors also suggest that while naphthalene can produce respiratory toxicity in rodents, such effects are most unlikely to be observed in humans. Levels of CYP2F expression in pulmonary and nasal tissues were found to be greater in the mouse and rat than in a non-human primate, with the levels of expression in rodents correlating with tissue susceptibility to naphthalene-induced toxicity /9/. Studies with lung microsomes have shown that rates of naphthalene metabolism are 10-100 times lower in human and non-human primate tissue preparations compared to mouse and rat lung microsomes /11,17/. Apart from higher rates of naphthalene bioactivation in rodents compared to humans, there also appear to be species differences in naphthalene detoxification. Microsomal epoxide hydrolase probably exhibits stereoselectivity for naphthalene epoxide hydrolysis, as has been shown for styrene oxide /44/. It is well established /45,46/ that while epoxide hydrolase is employed for epoxide hydrolysis in humans, rodents such as the rat and mouse utilize cellular reduced glutathione (GSH) which can become rapidly depleted in the process, thus leading to enhanced cellular toxicity in these species. Indeed, the depletion of GSH results in covalent binding of reactive naphthalene metabolites in mouse Clara cells, whereas tolerance to naphthalene-induced Clara cell toxicity is due to enhanced GSH synthesis /16,47/. The reported evidence indicates that the relative levels of epoxide hydrolase and GSH in rodent species and man are broadly consistent with the species differences in toxicity for naphthalene, and presumably for other compounds which are liable to become activated via epoxidation.

## CONCLUSIONS

Naphthalene is metabolically activated to the 1,2-epoxide by CYP2F enzymes in rat, mouse and man. This is most likely the cause of its respiratory tract toxicity, but the rate of formation, the stability of its epoxide (including the stereoisomer ratio) and the level of epoxide hydrolase involvement would appear to provide an explanation for the species differences in naphthalene toxicity between rodents and man. The detoxifying influence of CYP2A13, the human enzyme present in the respiratory tract, will almost certainly contribute significantly to the low overall degree of naphthalene toxicity in



humans, as opposed to the situation manifested in the two rodent species.

Comparison between naphthalene and coumarin metabolism and toxicity in the three mammalian species, rat, mouse and human, shows that the species differences may relate to cytochrome P450-mediated pathways. In particular, CYP2F1 is involved in naphthalene epoxidation in humans, whereas CYP2A13 and CYP2B6 generally detoxify this compound via the 1-hydroxylation pathway in the same species. CYP2A13 also mediates in the formation of 2-naphthol. For coumarin, it is CYP2A6 which mediates detoxication via 7-hydroxylation in man, whereas CYP1A2 and CYP2E1 tend to form the 3,4-epoxide which is the activating pathway /38,48/. These two enzymes are also present in rat and mouse (although their sequences differ slightly) where toxic activation is apparent in both rodent species. However, detoxification pathways are less apparent in these two rodent species than in man /41/. This is probably due to the fact that the CYP2A orthologues in rat and mouse do not readily metabolize coumarin, which thus represents a species difference relative to man. Consequently, further work is required to provide more definitive statements on the toxicity and species differences in certain CYP2F substrates, such as naphthalene.

#### ACKNOWLEDGEMENTS

The financial support of the Naphthalene Research Group Committee is gratefully acknowledged by one of us (DFVL). Yuko Ito would like to thank the Japanese Foundation for funding her PhD studentship at the University of Surrey.

#### REFERENCES

1. Furge LL, Guengerich FP. Cytochrome P450 enzymes in drug metabolism and chemical toxicology. *Biochem Mol Biol Educ* 2006; 34: 66-74.
2. Gibson GG, Skett P. *Introduction to Drug Metabolism*, 3<sup>rd</sup> Ed. Cheltenham: Nelson Thornes, 2001.
3. Gonzalez FJ, Gelboin HV. Role of human cytochromes P450 in the metabolic activation of carcinogens and toxins. *Drug Metab Rev* 1994; 26: 165-183.
4. Guengerich FP. Cytochrome P450 and chemical toxicology. *Chem Res Toxicol* 2008; 21: 70-83.

5. Timbrell JA. Principles of Biochemical Toxicology, 2<sup>nd</sup> Ed. London: Taylor & Francis, 1991.
6. Hewitt NJ, Lechon MJG, Houston JB, Hallifax D, Brown HS, Maurel P, Kenna JG, Gustavsson L, Lohmann C, Skonberg C, Guillouzo A, Tuschl G, Li AP, LeCluyse E, Groothuis GMM, Hengstler JG. Primary hepatocytes: current understanding of the regulation of metabolic enzymes and transporter proteins, and pharmaceutical practice for the use of hepatocytes in metabolism, enzyme induction, transporter, clearance and hepatotoxicity studies. *Drug Metab Rev* 2007; 39: 159-234.
7. Guengerich FP. Human cytochrome P450 enzymes. In: Ortiz de Montellano PR, ed. *Cytochrome P450*. New York: Kluwer/Plenum, 2005; 377-530.
8. Lewis DFV. Guide to the Structure and Function of Cytochromes P450. London: Taylor & Francis, 2001.
9. Baldwin RM, Jewell WT, Fanucchi MV, Plopper CG, Buckpitt AR. Comparison of pulmonary/nasal CYP2F expression levels in rodents and Rhesus macaque. *J Pharmacol Exp Ther* 2004; 309: 127-136.
10. Baldwin RM, Shultz MA, Buckpitt AR. Bioactivation of the pulmonary toxicants naphthalene and 1-nitronaphthalene by rat CYP2F4. *J Pharmacol Exp Ther* 2005; 312: 857-865.
11. Buckpitt A, Boland R, Isbell M, Morin D, Shultz M, Baldwin R, Chan K, Karlsson A, Lin C, Taff A, West J, Fanucchi M, Van Winkle L, Plopper C. Naphthalene-induced respiratory tract toxicity: metabolic mechanisms of toxicity. *Drug Metab Rev* 2002; 34: 791-820.
12. Carlson GP. Critical appraisal of the expression of cytochrome P450 enzymes in human lung and evaluation of the possibility that such expression provides evidence of potential styrene tumorigenicity in humans. *Toxicology* 2008; 254: 1-10.
13. Zhang Q-Y, Ding X. The CYP2F, CYP2G and CYP2J subfamilies. In: Ioannides C, ed. *Cytochromes P450: Role in the Metabolism and Toxicity of Drugs and other Xenobiotics*. Cambridge: Royal Society of Chemistry, 2008; 309-353.
14. Shultz MA, Choudary PV, Buckpitt AR. Role of murine cytochrome P450 2F2 in metabolic activation of naphthalene and metabolism of other xenobiotics. *J Pharmacol Exp Ther* 1999; 290: 281-288.
15. West JAA, Pakeham G, Morin D, Fleschner CA, Buckpitt AR, Plopper CG. Inhaled naphthalene causes dose dependent Clara cell cytotoxicity in mice but not in rats. *Toxicol Appl Pharmacol* 2001; 173: 114-119.
16. West JAA, Buckpitt AR, Plopper CG. Elevated airway GSH resynthesis confers protection to Clara cells from naphthalene injury in mice made tolerant by repeated exposures. *J Pharmacol Exp Ther* 2000; 294: 516-523.
17. International Agency for Research on Cancer (IARC). IARC Monographs on the Evaluation of Carcinogenic Risks to Humans, Volume 82. Some Traditional Herbal Medicines, Some Mycotoxins, Naphthalene and Styrene. Lyon: IARC Press, 2002.

18. North DW, Abdo KM, Benson JM, Dahl AR, Morris JB, Renne R, Witschi H. A review of whole animal bioassays of the carcinogenic potential of naphthalene. *Regul Toxicol Pharmacol* 2008; 51: S6-S14.
19. Cho TM, Rose RL, Hodgson E. In vitro metabolism of naphthalene by human liver microsomal cytochrome P450 enzymes. *Drug Metab Dispos* 2006; 34: 176-183.
20. Wang H, Lanza DL, Yost GS. Cloning and expression of CYP2F3, a cytochrome P450 that bioactivates the selective pneumotoxins 3-methylindole and naphthalene. *Arch Biochem Biophys* 1998; 349: 329-340.
21. Lewis DFV, Bailey PT, Low LK. Molecular modelling of the mouse cytochrome P450 CYP2F2 based on the CYP102 crystal structure template and selective CYP2F2 substrate interactions. *Drug Metab Drug Interact* 2002; 19: 97-113.
22. Wester MR, Johnson EF, Marques-Soares C, Dijols S, Dansette PM, Mansuy D, Stout CD. Structure of mammalian cytochrome P4502C5 complexed with diclofenac at 2.1 Å resolution: evidence for an induced fit model of substrate binding. *Biochemistry* 2003; 42: 9335-9345.
23. Gotoh O. Substrate recognition sites in cytochrome P450 family 2 (CYP2) proteins inferred from comparative analysis of amino acid and coding nucleotide sequences. *J Biol Chem* 1992; 267: 83-90.
24. Buckpitt AR, Cruikshank MK. Biochemical function of the respiratory tract: metabolism of xenobiotics. In: Roth RA, ed. *Comprehensive Toxicology*, Vol 8. Amsterdam: Elsevier, 1997; 159-186.
25. Czerwinski M, McLemore TL, Philpot RM, Nhamburo PT, Korzekwa KR, Gelboin HV. Metabolic activation of 4-ipomeanol by complementary DNA-expressed human cytochrome P450: evidence for species-specific metabolism. *Cancer Res* 1991; 51: 4636-4638.
26. Forkert PG, Baldwin RM, Millen B, Lash LH, Putt DA, Shultz MA, Collins KS. Pulmonary bioactivation of trichloroethylene to chloral hydrate: relative contributions of CYP2E1, CYP2F1 and CYP2B1. *Drug Metab Dispos* 2005; 33: 1429-1437.
27. Nakajima T, Elovaara E, Gonzalez FJ, Gelboin HV, Raunio H, Pelkonen O. Styrene metabolism by cDNA-expressed human hepatic and pulmonary cytochromes P450. *Chem Res Toxicol* 1994; 7: 891-896.
28. Nhamburo PT, Kimura S, McBride OW, Kozak CA, Gelboin HV, Gonzalez FJ. The human CYP2F gene subfamily: identification of a cDNA encoding a new cytochrome P450, cDNA-directed expression and chromosome mapping. *Biochemistry* 1990; 29: 5491-5499.
29. Powley MW, Carlson GP. Cytochromes P450 involved with benzene metabolism in hepatic and pulmonary microsomes. *J Biochem Mol Toxicol* 2000; 14: 303-309.
30. Ritter JK, Owens IS, Negishi M, Nagata K, Sheen YY, Gillette JR, Sasame HA. Mouse pulmonary cytochrome P450 naphthalene hydroxylase: cDNA cloning, sequence and expression in *Saccharomyces cerevisiae*. *Biochemistry* 1991; 30: 11430-11437.

31. Simmons AC, Reilly CA, Baldwin RM, Ghanayem BI, Lanza DL, Yost GS, Collins KS, Forkert PG. Bioactivation of 1,1-dichloroethylene to its epoxide by CYP2E1 and CYP2F enzymes. *Drug Metab Dispos* 2004; 32: 1032-1039.
32. Thornton-Manning J, Appleton JL, Gonzalez FJ, Yost GS. Metabolism of 3-methylindole by vaccinia-expressed P450 enzymes: correlation of 3-methyleneindolenine formation and protein binding. *J Pharmacol Exp Therap* 1999, 276: 21-29.
33. Rendic S. Summary of information on human CYP enzymes: human P450 metabolism data. *Drug Metab Rev* 2002; 34: 83-448.
34. Fukami T, Katoh M, Yamazaki H, Yokoi T, Nakajima M. Human cytochrome P450 2A13 efficiently metabolizes chemicals in air pollutants: naphthalene, styrene and toluene. *Chem Res Toxicol* 2008; 21: 720-725.
35. Carr BA, Wan J, Hines RN, Yost GS. Characterization of the human lung CYP2F1 gene and identification of a novel lung specific binding motif. *J Biol Chem* 2003; 278: 15473-15483.
36. Creighton TE. *Proteins: Structures and Molecular Properties*. New York: Freeman, 1993.
37. Martignoni M, Groothuis GMM, de Kanter R. Species differences between mouse, rat, dog, monkey and human CYP-mediated drug metabolism, inhibition and induction. *Exp Opin Drug Metab Toxicol* 2006; 2: 875-894.
38. Born SL, Caudill D, Fliter KL, Purdon MP. Identification of the cytochromes P450 that catalyze coumarin 3,4-epoxidation and 3-hydroxylation. *Drug Metab Dispos* 2002; 30: 483-487.
39. Born SL, Fix AS, Caudill D, Lehman-McKeeman LD. Selective Clara cell injury in mouse lung following acute administration of coumarin. *Toxicol Appl Pharmacol* 1998, 151: 45-56.
40. Felter SP, Vassallo JD, Carlton BD, Daston GP. A safety assessment of coumarin taking into account species-specificity of toxicokinetics. *Food Chem Toxicol* 2006; 44: 462-475.
41. Lake BG. Coumarin metabolism, toxicity and carcinogenicity. relevance for human risk assessment. *Food Chem Toxicol* 1999; 37: 423-453.
42. Born SL, Fix AS, Caudill D, Lehman-McKeeman LD. Development of tolerance to Clara cell necrosis with repeat administration of coumarin. *Toxicol Sci* 1999; 51: 300-309.
43. Zhuo X, Gu J, Zhang Q-Y, Spink DC, Kaminsky LS, Ding X. Bio-transformation of coumarin by rodent and human cytochromes P-450: metabolic basis of tissue-selective toxicity in olfactory mucosa of rats and mice. *J Pharmacol Exp Ther* 1999; 288: 463-471.
44. Carlson GP. Effects of inducers and inhibitors on the microsomal metabolism of styrene to styrene oxide in mice. *J Toxicol Environ Health* 1997; 51: 477-488.
45. Lorenz J, Glatt HR, Fleischmann R, Ferlinz R, Oesch F. Drug metabolism in man and its relationship to that in three rodent species: monooxygenase, epoxide hydrolase and glutathione S-transferase activities in subcellular fractions of lung and liver. *Biochem Med* 1984, 32: 43-56.

46. Kitteringham NR, Davis C, Howard N, Pirmohamed M, Park BK. Inter-individual and interspecies variation in hepatic microsomal epoxide hydrolase activity: studies with *cis*-stilbene oxide, carbamazepine 10,11-epoxide and naphthalene. *J Pharmacol Exp Ther* 1996; 278: 1018-1027.
47. Phimister AJ, Lee MG, Morin D, Buckpitt AR, Plopper CG. Glutathione depletion is a major determinant of inhaled naphthalene respiratory toxicity and naphthalene metabolism in mice. *Toxicol Sci* 2004; 82: 268-278.
48. Vassallo JD, Hicks SM, Born SL, Daston GP. Roles for epoxidation and detoxification of coumarin in determining species differences in Clara cell toxicity. *Toxicol Sci* 2004; 82: 26-33.
49. Lanza DL, Code E, Crespi CL, Gonzalez FJ, Yost GS. Specific dehydrogenation of 3-methylindole and epoxidation of naphthalene by recombinant human CYP2F1 expressed in lymphoblastoid cells. *Drug Metab Dispos* 1999; 27: 798-803.
50. Lewis DFV, Ito Y, Lake BG. Metabolism of coumarin by human P450s: a molecular modelling study. *Toxicol In Vitro* 2006; 20: 256-264.

